Chaos, Solitons & Fractals 44 (2011) 226–240

Contents lists available at ScienceDirect

Chaos, Solitons & Fractals

Nonlinear Science, and Nonequilibrium and Complex Phenomena

journal homepage: www.elsevier.com/locate/chaos

NAFASS: Discrete spectroscopy of random signals

R.R. Nigmatullin [a,*], S.I. Osokin [a,*], V.A. Toboev [b]

[a] Institute of Physics, Kazan (Volga Region) Federal University, Kremlevskaya str.18, Kazan, Tatarstan 420008, Russia
[b] Department of Mathematics, Chuvash State University, Moskovskiy pr.,15, Cheboksary 428015, Russia

ARTICLE INFO

Article history:
Received 27 December 2010
Accepted 4 February 2011
Available online 23 March 2011

ABSTRACT

In this paper we suggest a new discrete spectroscopy for analysis of random signals and fluctuations. This discrete spectroscopy is based on successful solution of the modified Prony's problem for the strongly-correlated random sequences. As opposed to the general Prony's problem where the set of frequencies is supposed to be unknown in the new approach suggested the distribution of the unknown frequencies can be found for the strongly-correlated random sequences. Preliminary information about the frequency distribution facilitates the calculations and attaches an additional stability in the presence of a noise. This spectroscopy uses only the informative-significant frequency band that helps to fit the given signal with high accuracy. It means that any random signal measured in *t*-domain can be "read" in terms of its amplitude-frequency response (AFR) *without* model assumptions related to the behavior of this signal in the frequency region. The method overcomes some essential drawbacks of the conventional Prony's method and can be determined as the non-orthogonal amplitude frequency analysis of the smoothed sequences (NAFASS). In this paper we outline the basic principles of the NAFASS procedure and show its high potential possibilities based on analysis of some actual NIR data. The AFR obtained serves as a specific fingerprint and contains all necessary information which is sufficient for calibration and classification of the informative-significant band frequencies that the complex or nanoscopic system studied might have.

1. Formulation of the problem

In spite of the essential progress of the Fourier and wavelet analysis [1–14] the treatment and subsequent fit of an arbitrary random sequence containing a set of unknown multi-frequency periodical functions is far from its satisfaction. For any researcher it is necessary to fit a segment of the given random sampling (or signal) by a finite number of frequencies with amplitudes that contain significant information about the periodical processes involved in its behavior. For example, in Fig. 1 we show a typical example of such kind containing a sufficient large number of the measured points ($N > 1500$). For this part of the random sequence it would be very important to find the desired fitting function, including only the informative-significant band of frequencies and amplitudes that can fit this segment with high accuracy. The first attempt of such kind was undertaken by Prony in 1795. During long period this method was essentially modified [15–30] but in nowadays many researchers admit that this method is *not* numerically stable for large number of measured points and to presence of a random component defined usually as "a noise". In order to overcome these drawbacks and increase the possibilities of the fitting of any random sequences one can try to achieve *preliminary* information about the frequency distribution $\omega_k\,(k = 0, 1, \ldots, K-1)$ over the numbers of modes k. If this information can be found

Abbreviations: ACF, autocorrelation function; AFR, amplitude–frequency response; ECs, the Eigen-Coordinate method; FM, fluctuation metrology; LLSM, the linear least-square method; LPSCV, the linear principle of the strongly correlated variables; NAFASS, non-orthogonal amplitude–frequency analysis of the smoothed sequences; NIR, near infra-red; PEN, pseudo-ergodic noise; POLS, procedure of the optimal linear smoothing.

* Corresponding authors.
E-mail address: nigmat@knet.ru (R.R. Nigmatullin).

0960-0779/$ - see front matter © 2011 Elsevier Ltd. All rights reserved.
doi:10.1016/j.chaos.2011.02.003

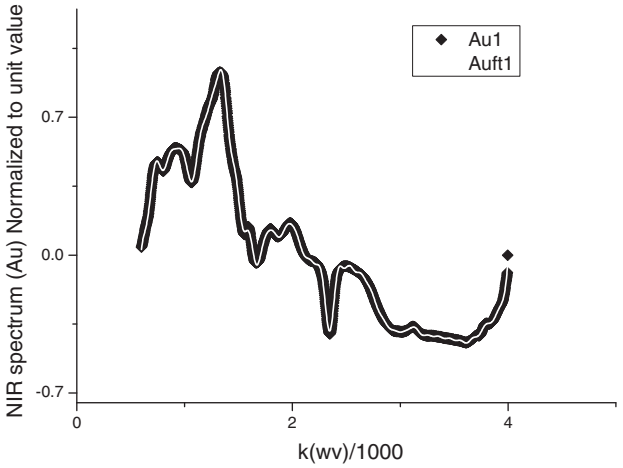

Fig. 1. The NIR spectrum of Au electrode and its fit (shown by white bold line) realized with the help of the NAFASS approach.

then the roots (that are associated with unknown frequencies) are easily found and all numerical procedure is facilitated essentially.

In this paper we are going to prove that the desired frequency distributions can be found for the strongly-correlated random signals $S(t)$. In other words, we are going to prove that for the strongly-correlated systems the fitting function

$$S(t) \cong F(t) = A_0 + \sum_{k=0}^{K-1} [Ac_k \cos(\omega_k t) + As_k \sin(\omega_k t)] \qquad (1)$$

(where ω_k ($k = 0, 1, \ldots, K-1$) defines the set of frequencies, Ac_k and As_k are the corresponding amplitudes) can be the first and probably unique candidate in solution of the fitting problem posed above. The unknown distributions of frequencies ω_k for the strongly-correlated systems should satisfy to the following relationships

$$\omega_k = \omega_{\min} + \frac{k}{K-1}(\Omega_{\max} - \omega_{\min}), \quad k = 0, 1, \ldots, K-1 \qquad (2)$$

$$\omega_k = \omega_{\min}\left(\frac{\Omega_{\max}}{\omega_{\min}}\right)^{\frac{k}{K-1}}, \quad k = 0, 1, \ldots, K-1 \qquad (3)$$

In relationships (2) and (3) the limits of the frequency band $[\omega_{min}, \Omega_{max}]$ and the number of limiting mode K are found from the original approach described below. We want to stress here that the fitting function (1) contains the set of periodical functions that are *not orthogonal* to each other. It is well-known that the fitting of the finite segment of random sequence in the form of a linear combination of periodical functions with different frequencies in the given temporal interval with acceptable accuracy represents a serious problem of the modern Fourier analysis. This problem also is the key point in solution of the Prony's problem. Directly this procedure can be realized in the frame of the Prony's method and initially it contains $3K + 1$ fitting parameters and the limits of the fitting frequencies $\omega_{min} \leqslant \omega_k \leqslant \Omega_{max}$ *a priory* are *not* known. Unfortunately, the Prony's method is not numerically stable and in spite of the essential efforts of many researches it does not receive a wide diffusion. The basic limitation is related to calculation of the eigen-values of the Grassman matrix [25–30]. The Prony's method is applicable when the following *priory suppositions* are fulfilled:

(a) The sequence $S(t)$ should contain obligatory at least one harmonic component;
(b) The constant component A_0 in (1) is absent;
(c) For stability purposes the number of components K in (1) satisfies approximately to condition $N/K \cong 3$. It means that the number of the measured points cannot be large and compression of the initial sequence is low.

This preliminary analysis of the drawbacks of the Prony's method allows us to formulate the modified problem that we are going to solve.

The NAFASS method should include the following attractive features:

1. It can be applicable for decomposition of *any* randomness with number of data points N entering into the given sequence not exceeding 1500. This limitation is not essential. But inside of this limit ($N < 1500$) the number of frequencies providing the fit of the given sequence with high accuracy satisfies to compression condition $N/K \leqslant 20$–30.
2. It should determine the minimal number of harmonic components K figuring in (1) In order to satisfy this condition the procedure of the optimal linear smoothing (POLS) can be applied. This procedure has been described in papers [31–33].
3. The fit of the given sequence $S(t)$ with the help of the function $S(t) \cong F(t)$ should provide the high accuracy. At least, the minimal value of the relative error should not exceed the units of percentages (Relerr < 5–9%).
4. In order to decrease the number of the unknown frequencies and facilitate the nonlinear fit their dependence from the mode k should be specified. At least the dependencies (2) and (3) can be found for the strongly-correlated variables. The justification of these expressions is given below.
5. The fit of the given sequence with the help of expression (1) should give a possibility to continue the fitting function $F(t)$ out of the given interval $[0, T]$. In other words, it should describe a random process in the intervals $[-\Delta, 0]$ and $[T, T + \Delta]$ ($\Delta > 0$).
6. As the final result of this decomposition it should give the dependencies $Ac_k(\omega_k)$ and $As_k(\omega_k)$ ($k = 0, 1, \ldots, K-1$) representing the AFR for further analysis and comparison of one random segment with another one.

As it has been mentioned above in order to make a problem more soluble it is necessary to reduce the number of unknown frequencies ω_k justifying their dependence over the index k. As it will be shown below one can justify the dependencies (2) and (3) and find the limiting frequencies $[\omega_{min}, \Omega_{max}]$ for both cases. We formulate also the linear principle for the strongly-correlated variables (LPSCV) which can classify the strongly-correlated dependencies and select them from others, where the dependence ω_k

from k cannot be found and remains unknown. So, the successful solution of this problem gives a chance to suggest a new approach for analysis of a wide set of various random sequences. We define this approach as the Non-orthogonal Amplitude-Frequency Analysis of the Smoothed Samplings (NAFASS) for the strongly-correlated variables, which enables to select an informative-significant band of frequencies $\omega_{min} \leqslant \omega_k \leqslant \Omega_{max}$ and amplitudes Ac_k, As_k ($k = 0,1,\ldots,K-1$) figuring in (1). The fitting function (1) found in the frame of the NAFASS approach for the segment in Fig. 1 is shown by a solid line.

2. Consequences of the strongly-correlated variables principle

In paper [34] one of the authors (RRN) formulated the Linear Principle for the Strongly-Correlated Variables (LPSCV) and found a possible hypothesis that can fit the unknown sequence of the ranged amplitudes with acceptable accuracy. We remind here the LPSCV: [34]

1. We form from two given random segments the sequences of the ranged amplitudes SRA ($y^{(p)}$) satisfying conditions: $y_1^{(p)} > y_2^{(p)} \cdots > y_N^{(p)}$ ($p = 1,2$).
2. If two SRA being plotted with respect to each other form a curve close to a straight line then we define these variables as the *strongly-correlated*

$$SRA(y^{(2)}) \cong a \cdot SRA(y^{(1)}) + b \tag{4}$$

Because of importance of this definition for the further analysis we should formulate the basic statements and necessary mathematical expressions. Let us suppose that an *event* (under event, for example, one can implicate a current measurement) is described by a segment of random sequence. If a present event is created presumably by the previous events taking place in the nearest past then one can write the following expression

$$F(t+sT) = \sum_{n=0}^{s-1} a_n F(t+nT) \tag{5}$$

The meaning of this expression is the following. The event that takes place in the segment of time sT, ($0 < t \leqslant T$) is formed presumably by the events that took place in the nearest past. The maximal value of the parameter $n = s$ determines *the depth of the correlation* between the last event $F(t+(s-1)T)$ counted off from the initial function $F(t)$. The value of T, as before, is associated with a period of time corresponding to one cycle of possible periodical repetition of the event considered. In complete analogy with Eq. (5) one can consider the self-similar events. They satisfy to the following functional equation

$$\begin{aligned} &F(t\xi^s) = \sum_{n=0}^{s-1} a_n F(t\xi^n) \text{ or} \\ &F(\ln t + s\ln\xi) = \sum_{n=0}^{s-1} a_n F(\ln t + n\ln\xi) \end{aligned} \tag{6}$$

As one notice from comparison of these expressions relationship (6) is mathematically equivalent to (5) because of transformation ($\ln(t) \to t$, $\ln(\xi) \to T$). In paper [34] we found the solution of functional Eq. (5)

$$F(t) = \sum_{n=1}^{s} E_n(t)\exp(\lambda_n t), \tag{7a}$$

where $E_n(t)$ represents a set of periodical functions with period T, i.e. $E_n(t \pm mT) = E_n(t)$ with integer number m from the interval $[1,s]$. For Eq. (6) the solution using the substitution ($t \to \ln(t)$) can be easily presented as

$$F(\ln t) = \sum_{n=1}^{k} E_n(\ln t)\exp(\lambda_n \ln t) \tag{7b}$$

The substitution of solution (7a) into (5) leads to the following algebraic equation for the unknown values λ_n. They are found as the roots of the characteristic polynomial

$$x^s - \sum_{n=0}^{s-1} a_n x^n = 0, \lambda_m = \frac{\ln(x_m)}{T}, \quad m = 1,2,\ldots,s \tag{8}$$

So, the solution of the general Eq. (7a) can include periodical functions that are contained in the complex-conjugated roots obtained from solution of Eq. (8). The periodical functions $E_n(t)$ entering into (7a) are *not* known but, as it has been done in papers [35,36], it can be expressed in the one-mode approximation (OMA). It means that this function approximately can be written as

$$\begin{aligned} E_n(t) &\cong a_n + b_n\cos\left(2\pi\langle m\rangle\frac{t}{T} - \varphi_n\right) \\ &\equiv a_n + b_n\cos\left(2\pi m\frac{t}{\langle T\rangle} - \varphi_n\right) \end{aligned} \tag{9}$$

where m defines a number of the leading oscillation mode, the values a_n, b_n and φ_n define some fitting constants. For further understanding we consider the simplest case ($s = 1$)

$$F(t+T_k) = b_k F(t) + c_k \tag{10}$$

The solution of this equation is found in [34] and can be expressed as

$$\begin{aligned} &F(t) = E_k(t)\exp\left(\frac{\ln b_k}{T_k}t\right) + \frac{c_k}{1-b_k}, \quad b_k \neq 1, \\ &F(t) = E_k(t) + b_k\frac{t}{T_k}, \quad b_k = 1, \\ &E_k(\omega_k t \pm 2\pi n) = E(\omega_k t). \end{aligned} \tag{11}$$

Here we took into account that periodical function can be presented in the form of linear combination of well-known periodical functions (9). We present this function in the from

$$\begin{aligned} &E(\omega_k t) = a_k + Ac_k\cos\left(\frac{2\pi k}{\langle T\rangle}t\right) + As_k\sin\left(\frac{2\pi k}{\langle T\rangle}t\right), \\ &\omega_k = \frac{2\pi k}{\langle T\rangle} = k\omega_0 \end{aligned} \tag{12}$$

From (12) it follows that the unknown frequency ω_k is proportional to the kth mode, which determines its maximal contribution to $E(\omega_k t)$. In expression (12) $\langle T\rangle$ determines the mean value of unknown period. Analyzing expression (12) one can conclude that a set of frequencies for the

strongly-correlated variables satisfy to relationship (2). Having in mind the solution of the functional equation for self-similar variables [34], we have the following expressions

$$F(t\xi_k) = b_k F(t) + c_k \tag{13a}$$

$$\begin{aligned} F(t) &= E_k(\ln t)\exp\left(\frac{\ln b_k}{\ln \xi_k}\ln(t)\right) + \frac{c_k}{1-b_k}, \quad b_k \neq 1 \\ F(t) &= E_k(\ln t) + b_k \frac{\ln t}{\ln \xi_k}, \quad b_k = 1 \\ E_k(\ln(t\omega_k) &\pm 2\pi n) = E(\ln(t\omega_k)) \end{aligned} \tag{13b}$$

Applying the same arguments that lead to relationship (2) and taking into account the replacement ($t \leftrightarrow \ln(t)$) one can easily derive the relationship

$$\ln\left(\frac{\omega_k}{\omega_{\min}}\right) = \frac{k}{K-1}\ln\left(\frac{\Omega_{\max}}{\omega_{\min}}\right), \quad k = 0,1,\ldots,K-1, \tag{14}$$

that is equivalent to relationship (3). So, for the strongly-correlated variables we found two possible distributions (2) and (3) for a set of unknown frequencies that can characterize the behavior of the strongly-correlated random segment.

The next important problem is to find the limiting values ω_{min}, Ω_{max}. For the finding of these unknown values we suggest the following procedure. Let us suppose that the given segment $S(t)$ determined in the measured points (t_j, $j = 1,2,\ldots,N$) can be approximately fitted by the function $y_0(t)$ containing only one frequency ω_0. This function satisfies to the differential equation

$$\frac{d^2 y_0(t)}{dt^2} + \omega_0^2 y_0(t) \equiv (D^2 + \omega_0^2)y(t) = c_0 \tag{15}$$

This differential equation with solution

$$y_0(t) = a_0 + ac_0\cos(\omega_0 t) + as_0\sin(\omega_0 t), \quad a_0 = c_0/\omega_0^2 \tag{16}$$

is transformed easily (with the help of double integration) to the basic linear relationship (BLR)

$$Y(t) = C_1 X_1(t) + C_2 X_2(t) + C_3 X_3(t) \tag{17}$$

where

$$\begin{aligned} Y(t) &= y_0(t) - \langle\ldots\rangle \\ X_1(t) &= \int_{t_1}^{t}(t-u)y_0(u)du - \langle\ldots\rangle \\ C_1 &= -\omega_0^2, \\ X_2(t) &= t^2 - \langle\ldots\rangle, \quad X_3(t) = t - \langle\ldots\rangle \end{aligned} \tag{18}$$

The constants C_2, C_3 figuring in (17) are not essential for further calculations and can be omitted. Applying the fit of the initial function $S(t)$ by the hypothesis (16) one can find the frequency ω_0 that is close to the minimal value ω_{min}. Let us suppose that the fitting function contains a linear combination of periodical functions with two frequencies ω_0 and ω_1

$$y = y_0 + y_1, \quad \ddot{y}_0 + \omega_0^2 y_0 = 0, \quad \ddot{y}_1 + \omega_1^2 y_1 = 0 \tag{19}$$

If the frequency ω_0 is supposed to be known then the BLR for the function $y(t)$ is expressed as

$$Y(t) = \sum_{k=1}^{4} C_k X_k(t) \tag{20}$$

where the functions figuring in (20) are determined as

$$\begin{aligned} Y(t) &= y(t) - \langle\ldots\rangle \\ X_1(t) &= \int_{t_1}^{t}(t-u)y(u)du - \langle\ldots\rangle, \quad C_1 = -\omega_1^2 \\ X_2(t) &= t - \langle\ldots\rangle \\ X_3(t) &= \cos(\omega_0 t) - \langle\ldots\rangle, \quad C_3 = \frac{\omega_1^2 - \omega_0^2}{\omega_0^2}Ac_3 \\ X_4(t) &= \sin(\omega_0 t) - \langle\ldots\rangle, \quad C_4 = \frac{\omega_1^2 - \omega_0^2}{\omega_0^2}As_3 \end{aligned} \tag{21}$$

Application of expressions (21) to the segment $S(t)$ shows that the first calculated frequency always less in comparison with the second one $\omega_0 < \omega_1$. The results close to these calculations we obtain also in the case when we apply these formulae to the remnant function which is defined as the difference $Rm(t) = S(t) - y(t)$. These preliminary results can be easily explained if we notice that integration of expression (1) containing a set of frequencies always suppress the terms containing the largest ones. So, the usage of the eigen-coordinates (ECs) method [37–40] for calculation of unknown frequencies (which initially are not known) can give a possibility to find the low-frequency value ω_0 close to the desired minimal value $\omega_0 \approx \omega_{min}$. Similar results we should obtain from the differential equation of the fourth order containing two unknown frequencies

$$\left(D^2 + \omega_1^2\right)\left(D^2 + \omega_0^2\right)y(t) = c_0 \quad D \equiv \frac{d}{dt} \tag{22}$$

For calculation of the maximal value Ω_{max} we present the current frequencies in the form

$$\begin{aligned} \omega_k(b) &= \omega_{\min} + \frac{k}{K-1}(\omega_1 b - \omega_{\min}), \quad k = 0,1,\ldots,K-1 \\ \omega_k(b) &= \omega_{\min}\left(\frac{\omega_1 b}{\omega_{\min}}\right)^{\frac{k}{K-1}} \end{aligned} \tag{23}$$

Here $\omega_1 > \omega_0$ defines a seed (inoculating) frequency which is calculated from expressions (21) or (22). Considering b as the unknown fitting parameter one can apply function (1) for the fitting of the given segment $S(t)$. The verification on model files show that the relative error defined by expression

$$RelErr(K,b) = \left(\frac{stdev(S(t) - F(t,K,b))}{mean|S(t)|}\right)\cdot 100\% \tag{24}$$

and considered as the function of two variables b and K always has a local minima. From numerous minimal values that function (24) might have we should choose the deepest one that is located in the vicinity of the minimal frequency ω_{min}. The existence of this minimal point of function (24) is related to the *saturation phenomenon* when increasing of number of periodical functions with high

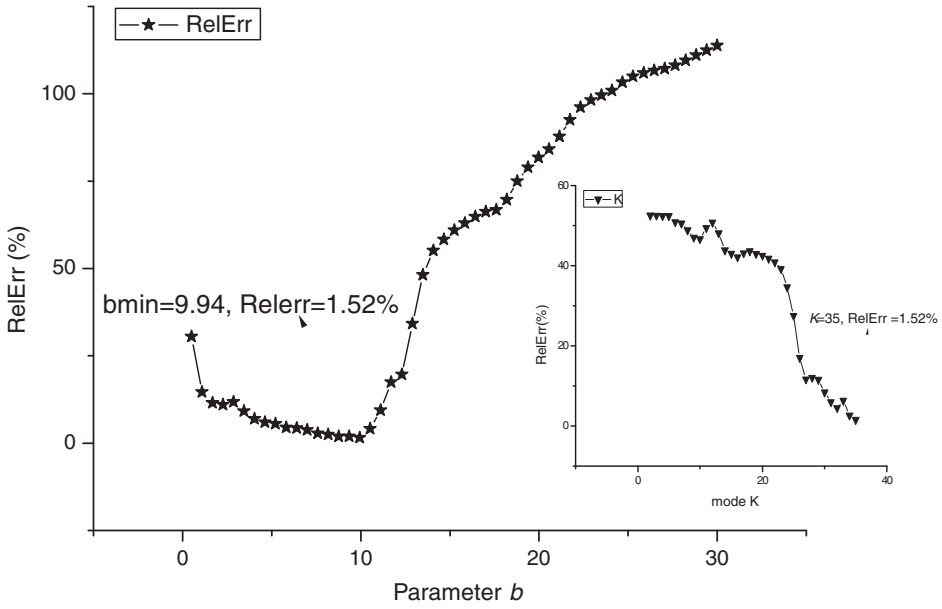

Fig. 2. Here we show the cross section of the relative error surface (Eq. (24)) corresponding to the minimal value of b and K. These calculated values ($b = 9.94$, $K = 35$) provide the optimal fit of the curve (shown on 1) with the value of the relative error less than 3%.

frequencies leads to *decreasing* the values of the corresponding amplitudes Ac_k, As_k. So, their contribution to the fitting of the given $S(t)$ becomes negligible. The behavior of the relative error (24) with respect to the parameter b at the given value of K is shown in Fig. 2. The minimal value of the first local minima b_{opt} counted off from the ω_{min} determines the desired value of the $\Omega_{max} = \omega_1 b_{opt}$. In such a way for the strongly-correlated variables satisfying to the LPSCV we realize the decomposition of the given random segment $S(t)$ on a set of the non-orthogonal periodical functions with informative-significant band of frequencies figuring in (1). In Fig. 3 we show the desired set of amplitudes Ac_k, As_k and the range of significant frequencies ω_k that provide the desired fit (shown on Fig. 1 by solid line) with the help of 35 frequencies and relative error less than 2%.

In practical applications of distributions (2) and (3) there is a problem to find number of exponents and differentiate a possible exponential solution from the power-law solution that follows as a solution of functional Eq. (6).

For solution of this problem one can apply the ECs method mentioned above. The applications of the ECs method for solution of some nontrivial problems were described in papers [38,40]. Here one can remind some peculiarities of the ECs method that makes it really attractive in different practical applications:

1. In the ECs method the problem of non-linear fitting of the exponential and power-law functions is reduced to the linear least square method (LLSM) that was properly investigated in many mathematical books related to the statistical problems. See, for example the book [41].
2. It does not require the guess of the fitting parameters and the final fit corresponds to the global minima in the space of the fitting parameters.

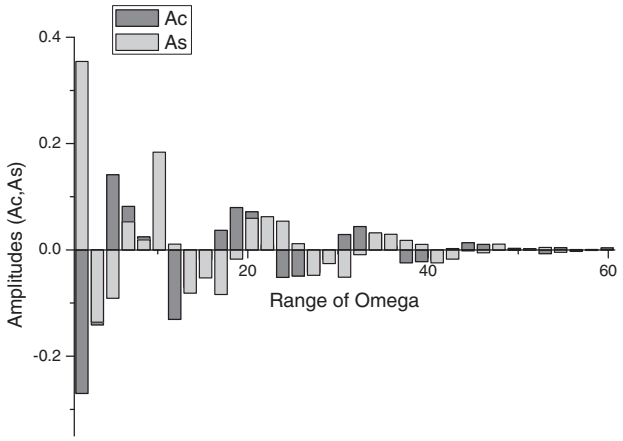

Fig. 3. The AFR corresponding to the fitting function shown in Fig. 1. This calculated distribution of amplitudes $Ac(\Omega_k)$, $As(\Omega_k)$ entering into the fitting function (1) is plotted against the frequency band occupying the interval $1.59 \leqslant \Omega_k \leqslant 59.87$.

3. The number of exponents (or power-law functions) can be found from the recognition procedure and minimization of the value of the standard deviation that is calculated for the difference between the segment of the random sequence and its fitting function.

The approach outlined above leads to one important conclusion. *Any* random function that can describe a behavior of one parameter with respect to the current variable (in most cases this parameter coincides with time) has at least *two* fitting functions. One function containing a minimal set of the fitting parameters follows from the specific model considered, another fitting function can follow from the LPSCV and in accordance with this principle it is described by a linear combination of exponential or power-law functions. For the cumulative curves (that is obtained by direct integration) the num-

ber of the fitting parameters is about 10. As for the fitting function $F(t)$ presented by expression (1) in order to provide the satisfactory fit (RelErr $(K,b) < 5$–9%) the required number of the significant frequencies is about 30–50 for the segments having 1000–2000 measured points. But in the case of absence of adequate model this fit (defined above as the NAFASS approach) is necessary for description of different complex systems (random series related to economical data, biomedical data, geophysical data and etc.) where suggestion of an adequate model presents a serious problem. This NAFASS approach is rather general and can be applicable for calculation the desired amplitude-frequency responses (AFR). The value of the smoothing window should be close to the optimal one and it is calculated with the accordance the procedure of the optimal smoothing (POLS) that is described in detail in the previous papers [31–33]. Function (1) in comparison with other fitting functions containing a sufficient number of the fitting parameters can be easily interpreted because the AFR functions $Ac_k(\omega_k)$, $As_k(\omega_k)$ have a clear meaning and can serve as very sensitive and specific "finger-prints" differentiating one quasi-periodical sequence from another one.

3. NAFASS and new discrete spectroscopy

As it is known from the linear response theory [42] the average value of some physical value $\langle A(t)\rangle$ is expressed by the relationship

$$\langle A(t)\rangle = \langle A\rangle_0 + \chi'(\omega)\cos(\omega t) + \chi''(\omega)\sin(\omega t) \tag{25}$$

where the real and imaginary components of the complex susceptibility at the fixed frequency

$$\chi(i\omega) = \chi'(\omega) - i\chi''(\omega) \tag{26}$$

are related to the pair correlation function

$$K(t) = i\langle[A(t),B]\rangle_0 = iQ^{-1}Sp(e^{-\beta H}[A(t),B]) \tag{27}$$

by the usual Fourier-transformation

$$\begin{aligned} K(t) &= \int_{-\infty}^{\infty}\chi(i\omega)e^{i\omega t}d\omega \\ &= \int_0^{\infty}[\chi'(\omega)\cos(\omega t) + \chi''(\omega)\sin(\omega t)]d\omega \end{aligned} \tag{28}$$

Here we took into account that $\chi(i\omega) = \chi'(\omega) - i\chi''(\omega)$, $\chi'(\omega) = \chi'(-\omega)$, $\chi''(\omega) = -\chi''(-\omega)$. From expression (28) it follows one important conclusion. Instead of having the total set of frequencies one can try to select the finite set of informative-significant frequencies located in the unknown frequency band and replace (28) by the finite segment of the Fourier-series

$$K(t) \cong A_0 + \sum_{k=0}^{K-1} Ac_k\cos(\omega_k t) + As_k\sin(\omega_k t) \tag{29}$$

where the number of modes (K) and the limits of the frequency band (ω_{min}, Ω_{max}) can be found from the NAFASS approach outlined above. Let us suppose that the physical value $A(t)$ corresponds to a random process measured experimentally (for example, it can be current $J(t)$, voltage $V(t)$ or charge $Q(t)$ fluctuations). For some stationary ergodic process the pair autocorrelation function can be calculated as

$$K_{AA}(t) = \lim_{T\to\infty}\frac{1}{T}\int_0^T A(t')A(t'+t)dt6' \cong^{N>>1} \left(\frac{1}{N-m}\right)\sum_{j=1}^{N-m}A_jA_{j+m} \tag{30}$$

for all $m = 0,1,\ldots,N-1$. So, in accordance with ergodic hypothesis one can assert that the correlation function calculated in accordance with the rules of the conventional statistical mechanics (the left side of (31)) should coincide for large samplings ($N \gg 1$) with autocorrelation function calculated with the rules of mathematical statistics (right side of (31))

$$\begin{aligned} K(t) &= i\langle[\Delta A(t),\Delta A]\rangle_0 \\ &\cong \lim_{N\to\infty}\left(\frac{1}{N-m}\right)\sum_{j=0}^{N-m}\Delta A_j\Delta A_{j+m}, \quad m = 0,1,\ldots, \quad \frac{N}{2} \end{aligned} \tag{31}$$

In particular, when $A(t) = J(t)$, ($J(t)$ is a random thermal current value) and taking into account the Nyquist relationship [42]

$$Re(\sigma_{\alpha\alpha}(\omega)) = \frac{\tanh(\omega/2\theta)}{\omega}K_{\alpha\alpha}(\omega) \tag{32}$$

one can obtain its discrete analog

$$\begin{aligned} K_{\alpha\alpha}(t) &\cong K_0 + \sum_{k=0}^{K-1}\left(K'_{\alpha\alpha}(\omega_k)\cos(\omega_k t) + K''_{\alpha\alpha}(\omega_k)\sin(\omega_k t)\right) \\ &= \sum_{k=0}^{K-1}\frac{\omega_k}{\tanh(\omega_k/2\theta)}\left(\sigma'_k(\omega_k)\cos(\omega_k t)\right. \\ &\quad \left. + \sigma''_k(\omega_k)\sin(\omega_k t)\right) \end{aligned} \tag{33}$$

that can be useful for the purposes of discrete spectroscopy. Expressions (32) and (33) open new possibilities of the discrete spectroscopy that is based on the replacement of the total Fourier spectrum by its finite frequency band containing only informative-significant components. We want to stress here again that these possibilities appear from the successful solution of the general Prony's problem, when the distributions of the frequency modes (2) and (3) for the strongly-correlated systems are *known*. This observation helps to solve the ill-posed Prony's problem [15–21] and describe any random signal in the form of expression (1) with high accuracy. So, the description of any random signal is reduced to analysis of its AFR that represents itself a specific "piano", where any discrete frequency of the AFR "sounds" with its peculiarities of the complex system analyzed. As it is well-known that for pure ergodic noise the pair auto-correlation function (ACF) defined by Eq. (31) is monotonic and satisfies to condition

$$K_0 > K_1 > \cdots > K_{N/2} \tag{34}$$

In real calculations this condition is violated and for short samplings the behavior of the ACF can have oscillating character or even accept the negative values. In order to

satisfy to condition (34) we should choose only decaying parts of random signals figuring in (31). So, dealing in reality with relatively short samplings ($N \cong (1500–2000)$ measured points) one can select only decaying parts and rectifying the increasing parts of the random signals which violate condition (34). This correction related to the fact that for very long samplings the contribution of "wrong" parts is becoming negligible but for the short samplings these wrong parts of random signals should be corrected. The noise which is obtained by such a way (by the procedure of selection of decaying parts and correction of increasing parts) from the given sampling we define as a pseudo-ergodic noise (PEN). We tested this procedure for available heat noise. For long samplings ($N \cdot \cong 10^6$–$2\ 10^6$) the contribution of "wrong" parts are really small but with decreasing of $N \cong (1500–2000)$ the number of wrong parts presenting in the random signal are increasing. So, the PEN helps to read the remnant noise in terms of possible fitting parameters belonging to the ACF. The details of this possibility are given in the next section.

4. Example based on real data

In paper [32] we demonstrated how to read NIR data in the frame of new data treatment approach. Here we want to demonstrate the general steps that should be applied to any "noisy" spectra that are registered by modern equipment on nanoscopic level. All treatment procedure can be divided on three basic parts.

1. The usage of the POLS for the initial digitized spectroscopic signal. This procedure helps to divide the initial signal on the optimal trend and the remnant "noise". Schematically it can be expressed in the form

$$POLS(nin(x_j)) = tr(x_j) + Rm(x_j), \quad j = 1, 2, \ldots, N, \tag{35}$$

   where $tr(x_j)$ is the smoothed spectrum (optimal trend) and $Rm(x_j)$ defines the remnant function (usually it is considered as a "useless noise" that is not used for further analysis).
2. After this separation one can apply the NAFASS to the function $tr(x_j)$ This approach is expressed schematically as

$$NAFASS[tr(x_j)] = [Ac(\omega_k), As(\omega_k)], \quad k = 0, 1, \ldots, K-1 \tag{36}$$

   This procedure helps to compress the initial spectrum $N/K \cong 20 \div 40$and read it in terms of the corresponding AFR.
3. In order not to lose any information from the initial noisy spectroscopic signal $nin(x_j)$ one can express the detrended function $Rm(x_j)$ in terms of the β-distribution function (see details in paper [43]) or in terms of the fitting parameters ACF, describing the pair correlation of the PEN (see the previous section for details). This procedure helps to receive (in the frame of controllable error) additional fitting parameters associated with the remnant function.

Let us apply these three general treatment steps for analysis of NIR spectra of Mercaptophenyl Diazonium Nanofilms (MDN) adsorbed on golden (Au) electrodes. All experimental part has been described in paper [32]. Here we select only three MDN measured spectra in order to show how to apply these basic treatment steps for "reading" of "noisy" spectra in general case. We show only minimal number of figures in order not to jam the content of the paper by excess details.

Step 1. In Figs. 4a, 4b, and 4c we show the application of the POLS for calculation of the smoothed spectra. In order to find the value of the optimal smoothing window ($0.08 < w < 0.1$) the POLS is applied for the *integrated* curves. The undoubted merits of such modification are discussed in paper [44].

Step 2. The second step is application of the NAFASS approach for calculation the desired AFR. In Figs. 5a and 5b we demonstrate the quality of the fitting procedure obtained for the smoothed NIR spectra. The calculated AFRs for these NIR spectra related to the behavior of the MDN absorbed of the surface of Au electrode are shown correspondingly on Figs. 6a and 6b. Even a simple analysis realized with the help of the NAFASS approach helps to notice some interesting features in behavior of the calculated AFRs. Two spectra have monotonic behavior with respect to amplitudes ($Ac(\Omega_k)$, $As(\Omega_k)$ ($k = 0, 1, \ldots, K-1$), $K = 40$) but with amplitudes that exceeds the values of initial spectra in 10^5 times. The AFR calculated for the third spectra reminds the random behavior. The explanation of these peculiarities related to the "physics" of this phenomenon merits more detailed research. Some basic parameters of these AFRs are collected in Table 1.

Step 3. The last step is related to analysis of the PEN and a possible fitting of the ACF defined by (31). The

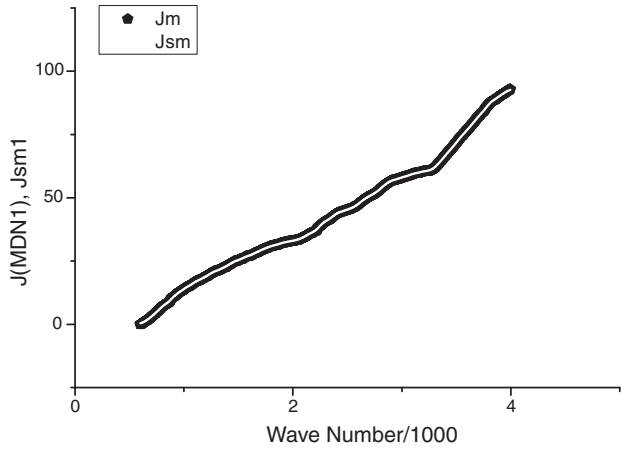

Fig. 4a. This figure shows the application of the POLS to integrated curve that represents the first NIR spectrum describing the absorption of MDN on Au electrode. Integrated curve is less deviated and facilitates in funding the value of the optimal smoothing window ($w = 0.081$). The optimal trend obtained by differentiation of this integrated trend (depicted by the white bold line) is shown below on Fig. 4b.

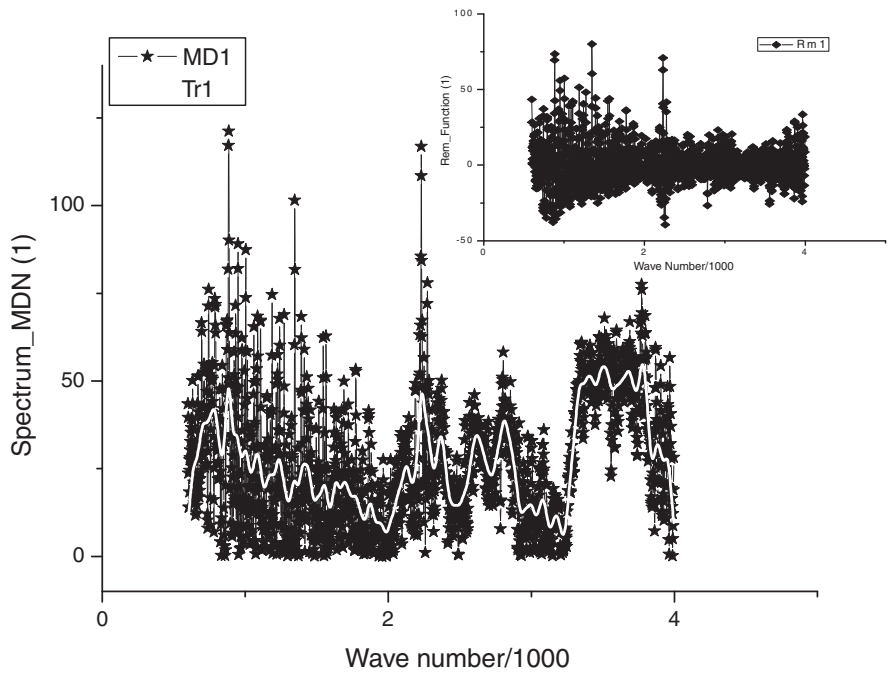

Fig. 4b. The smoothed spectrum (optimal trend) obtained by differentiation of the integrated trend is shown by white bold line. The remnant function (obtained by subtraction of the smoothed spectrum from initial noisy spectrum (black stars)) is shown on the small frame above. This remnant function will be analyzed in terms of the fitting parameters belonging to the calculated ACF.

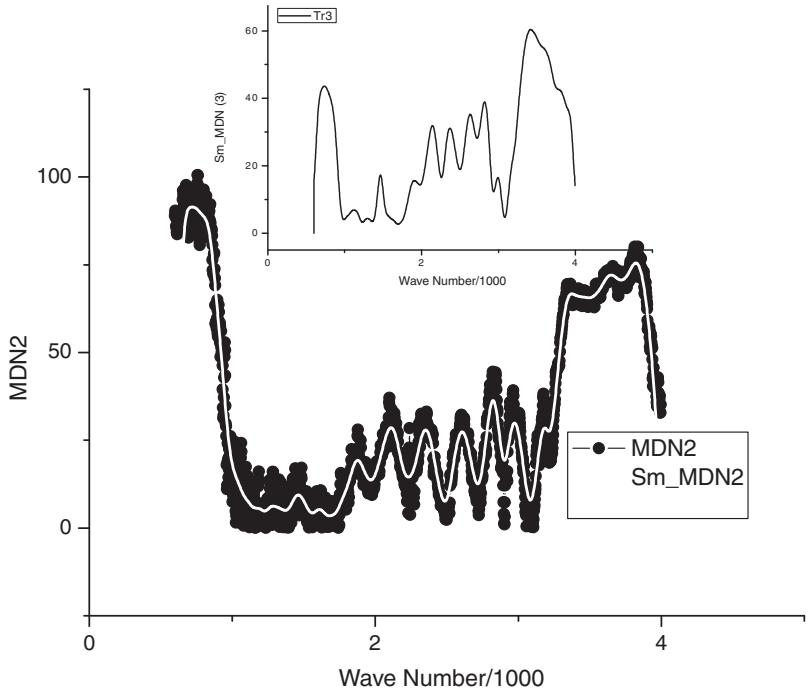

Fig. 4c. The same procedure is realized for two other MDN spectra. The results are shown here. The calculated NIR spectra for the MDN (2,3) are shown by white (on the main figure) and black (on the small figure above) solid lines correspondingly.

calculated auto-correlations functions are shown on Fig. 7a. They have monotonic behavior and usually occupy only 50% from the total set of the measured points ($N = 1762$). This peculiarity is related to the fact that zero points separating decreasing and increasing parts of the remnant function are equaled approximately to half points ($N/2$) from the total number N. This tendency is conserved for a sampling having an arbitrary length. The next problem is to find the optimal fitting function that enables to describe the monotonic behavior of the calculated ACFs. For

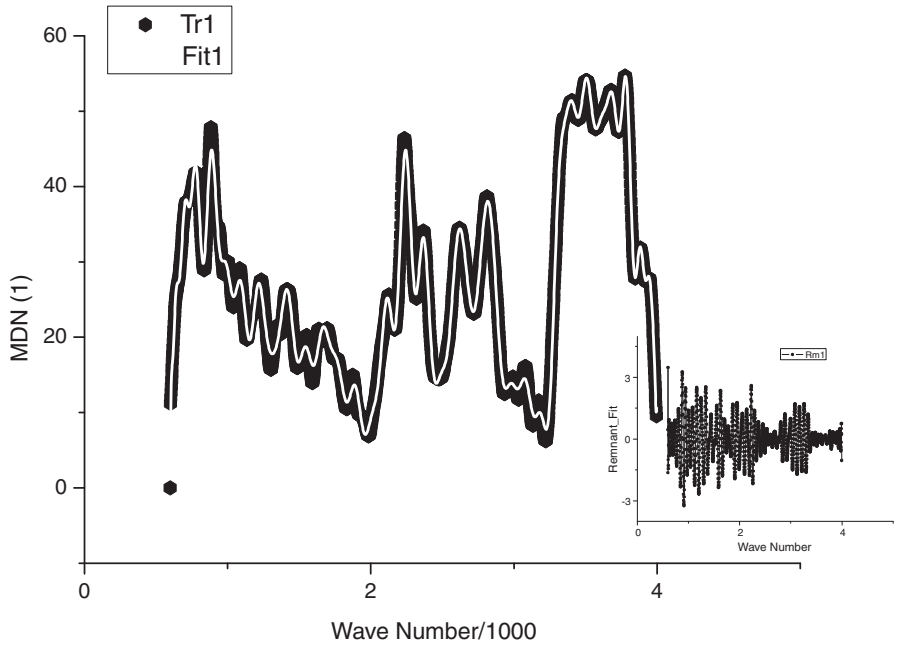

Fig. 5a. Here we show the results of the fitting procedure to Eq. (1) obtained for MDN (1). The values of the relative error and the Pearson correlation coefficients are collected in Table 1. In the small frame below we demonstrate the remnant function. If it is necessary it can be fitted also with subsequent analysis of its AFR.

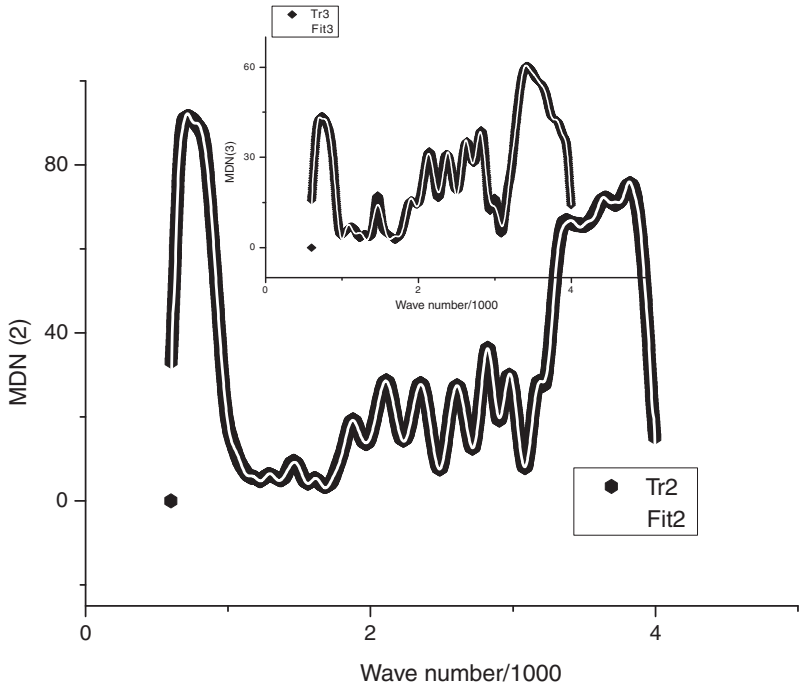

Fig. 5b. In the same manner we applied the NAFASS for the fitting of other two spectra MDN (2,3). The values of the relative error and the Pearson correlation coefficients are collected in Table 1.

solution of this problem we checked three possible hypotheses

$$K(t) = \sum_{s=0}^{S-1} a_s \cdot \exp(-\lambda_s \cdot t), \quad (a)$$
$$K(t) = \frac{1}{1 + \sum_{s=0}^{S-1} a_s \cdot \exp(v_s \cdot \ln(t))}, \quad (b) \qquad (37)$$
$$K(t) = \frac{1}{1 + \sum_{s=0}^{S-1} a_s \cdot \exp(v_s \cdot t)}, \quad (c)$$

The criteria of selection of the possible hypothesis are the following:

1. Identification with the help of the ECs method (correspondence to a set of straight lines [37,38])
2. The minimal number of components (S) that can enter into the summation sign.
3. The minimal value of the relative error at minimal value of the fixed S.

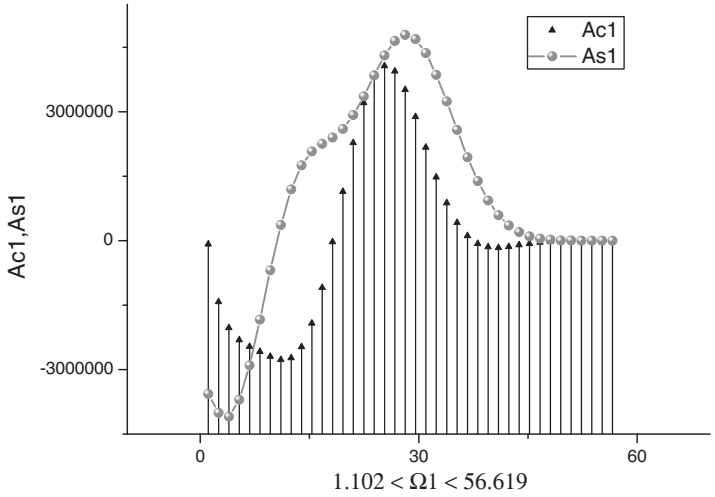

Fig. 6a. The desired AFR obtained for the first NIR spectra belonging to the MDN (1). The calculated AFR has a monotonic behavior. The most unexpected result is related to the values of amplitudes belonging to this decomposition. They exceed the values of initial NIR spectra in 10^5 times. This interesting behavior merits a special analysis.

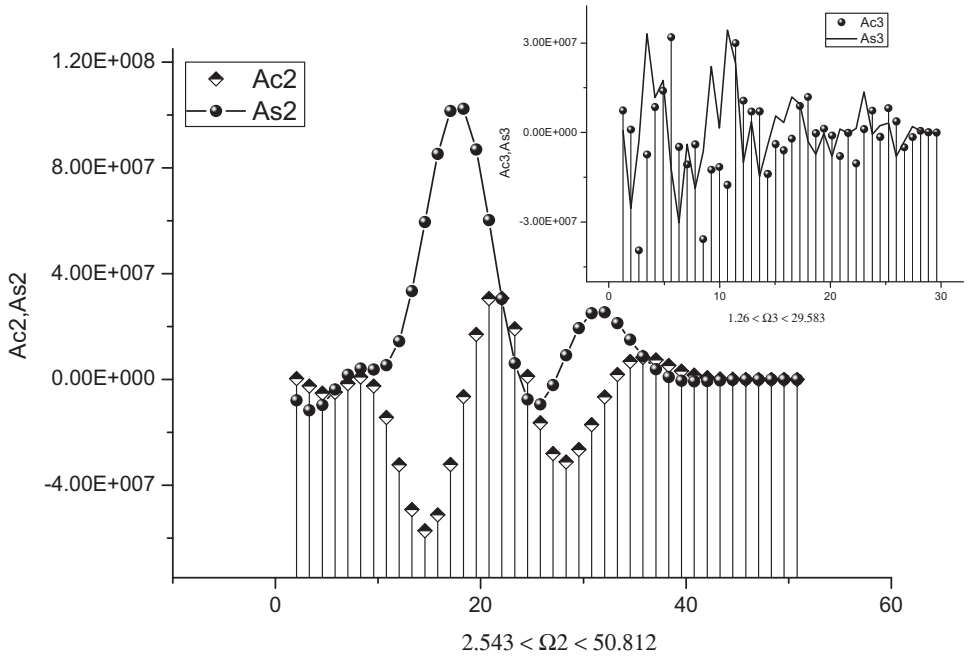

Fig. 6b. The calculated AFRs for the MDN (2,3). The order of magnitudes is conserved but behavior is different. For the third spectrum (depicted in the small frame above) the behavior is becoming random. So, the preliminary analysis of the corresponding AFRs helps to notice some peculiarities that can be obtained only within the NAFASS approach.

Table 1
The quantitative parameters characterizing AFR. Range of the value A is defined as Range $A = [\max(A) - \min(A)]/\mathrm{mean}(A)$.

Number of the ACF	ω_{min}	Ω_{max}	A_0	Range *Ac*, 1	Range *As*	RelErr (%)
1	1.10225	56.6192	1.39369E6	60.4595	8.86198	3.69022
2	2.05426	50.8119	−2.37777E6	−13.9959	6.82224	1.63977
3	1.25919	29.5829	−3.38691E7	−4.39331	2.92948	5.9222

We should omit some details in recognition procedure (identified also with separation procedure, described in papers [38–40]). The most probable hypothesis that satisfies to these criteria is the hypothesis (c). Some details of separation procedure are shown on Fig. 7a. The final fit is shown on Fig. 7b. The fitting parameters are collected in Table (2).

5. How "to read" a random signal describing some complex system? The basic principles of fluctuation metrology

In this paper we suggest a new type of spectroscopy that can find a wide application in analysis of quantum, heat and other fluctuations associated with any "event"

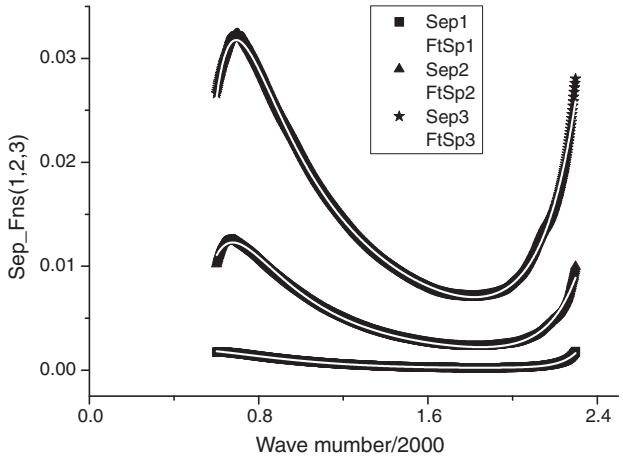

Fig. 7a. Here we show the fit for the inverse correlation functions associated to hypothesis (c) that is realized with the help of linear combination containing four exponents. This additional fit shows that the exponential separation procedure is correct. Besides it helps to calculate correctly the minimal value of the amplitude that enters into the linear combination of exponential functions.

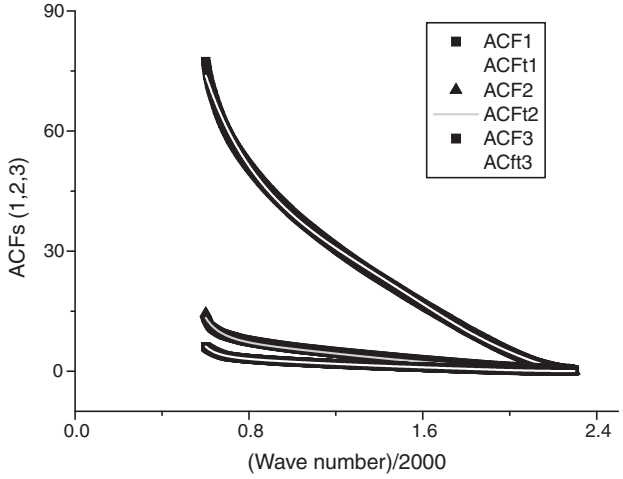

Fig. 7b. Here we show three ACFs calculated from the remnant noise and satisfying to the pseudo-ergodic hypothesis. The fitting functions satisfying to hypothesis (c) from Eq. (37) are shown by white bold lines. The fitting parameters related to this hypothesis are collected in Table 2.

that one can meet on submolecular and nanoscale levels. In order to convince the skeptically tuned reader in a high potential level of the NAFASS approach as the key element in analysis of a random signal describing some complex system let us repeat the basic elements that allow to read and compare random signals recorded from some complex biological object. The brief description of the biological data that will be analyzed below contains the following information:

1. The neurophysiologic experiments were realized on the slices of the spinal marrows of the young rats having 9–20 days age.
2. The thickness of each slice was 300 μm. Micropipette by means of electric circuit at the given negative voltage (−65 mV) connected the sensor neuron with container of a cell and only the spontaneous microcurrents coming through the cell membranes are recorded.
3. In order to support the living activity of the brain cells the temperature (20–23 °C) and the high level of oxygen are conserved during the whole period of the current registration (2–4 h).

Omitting other details that are important for the specialists of neurophysiology (these details can be important for the publication in the specialized journal) let us consider these microcurrents as a random sequence that can be read in terms of the NAFASS approach outlined above.

Three basic treatment steps (**S1**–**S3**) that were described in the previous section one can use for the "reading" of any random sequence (here we want to stress again *without* any model assumptions imposed on the random sequence considered) and its possible classification

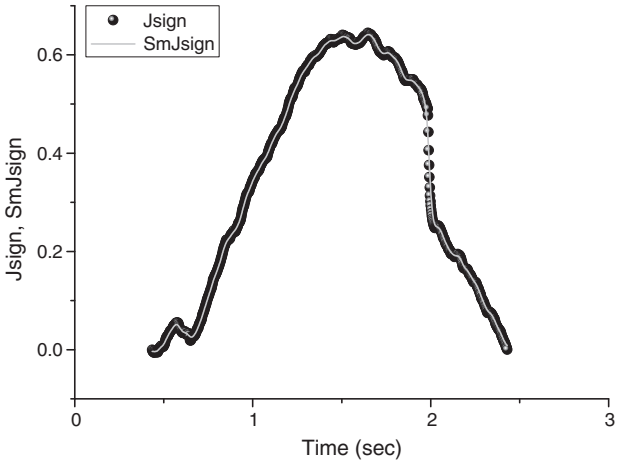

Fig. 8a. Here we show the integrated initial sequence (see Fig. 8b) and the smoothed trend (grey solid line) obtained in the frame of the POLS. The value of the optimal smoothing window is equaled to 0.03. W_{opt} provides the minimal value of the relative error.

Table 2
The fitting parameters describing the ACF (Eq. (37c)) $K(t) = \frac{K_0}{1+\sum_{s=1}^{4} A_s \cdot \exp(\lambda_s t)}$.

Number of the ACF	K_0	A_1, λ_1	A_2, λ_2	A_3, λ_3	A_4, λ_4	RelErr (%) PCC
1	6.6071	−4.0886E−4	−1.037	5.9525E−5	9.1185E−17	0.03927
		2.2243	−0.219	4.8524	17.355	0.99982
2	8.9014	−1.2042E−4	−34.331	0.05187	3.7336E−9	0.06055
		3.3886	−6.8275	2.4913	10.458	0.99959
3	5.1401	−1.2574E−4	−143.1	0.15371	9.5772E−8	0.02695
		3.5938	−8.858	2.0449	9.1177	0.99992

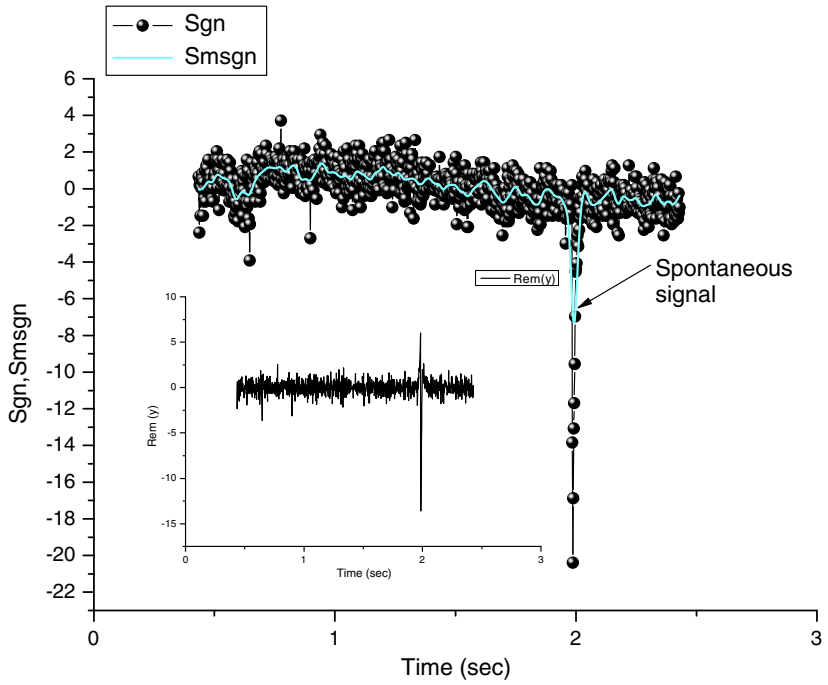

Fig. 8b. The initial signal (shown by connected black balls) and the calculated optimal trend (solid blue line). The "Sgn" and "Sm_sgn" data files describe microcurrents registered from membrane cell and multiplied in 10^3 times for clarity. The initial remnant function *Rem*(*y*) is obtained in accordance with expression (35) and shown below in the small frame. (For interpretation of the references to colour in this figure legend, the reader is referred to the web version of this article.)

for purposes of the fluctuation metrology (FM). This term was introduced in paper [45] by Prof. Timashev but the solution presented in [45] is unsatisfactory. Many stages contain uncontrollable errors, artificial suppositions and, from our opinion, this scheme cannot be used as a universal tool for metrological purposes. More simple and error-controllable approach presented in this paper can be used as a precise tool for the future FM. This approach containing only three simple steps is very general and it can be applied for consideration of a wide class of different fluctuations and the smoothed trends (signals) located inside the random sequence analyzed. In order to attract attention of a wide audience of the specialists studying a complexity and add some convincing arguments for the

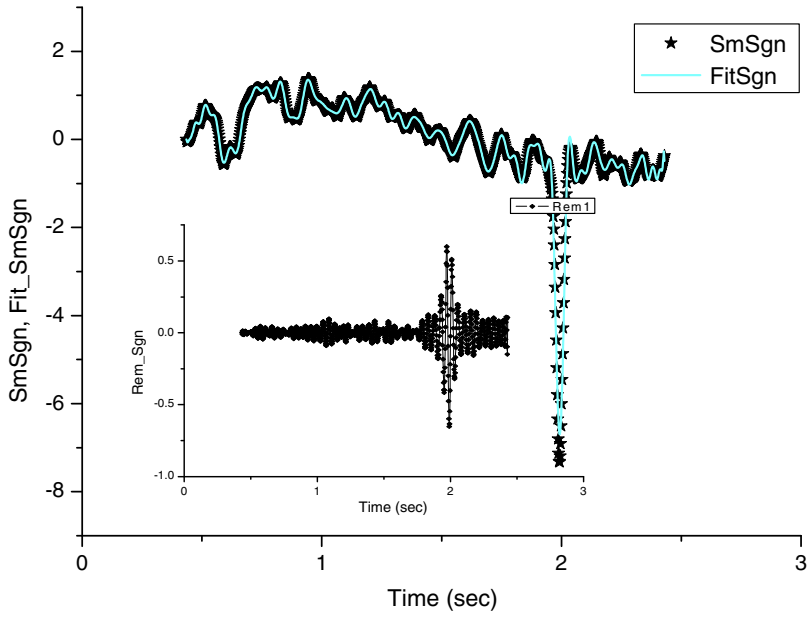

Fig. 9a. Here we show the fit (shown by solid blue line) of the optimal trend realized in the frame of the NAFASS. Another remnant function (do not mix with initial remnant function *Rem*(*y*)) "Rem_Sgn" (obtained as the difference between the optimal trend and its fitting function) is shown below in the small frame. (For interpretation of the references to colour in this figure legend, the reader is referred to the web version of this article.)

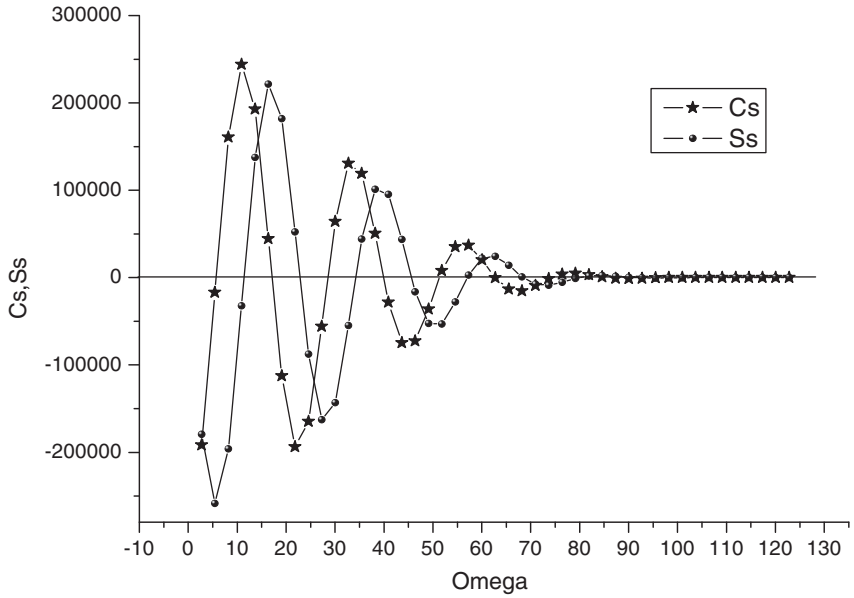

Fig. 9b. Here we show the AFR (1) that corresponds to the description of the optimal trend. It is interesting to note that the values of the calculated amplitudes exceed the fitting values in 10^5 times and have monotonic behavior. This specific behavior needs further research. The limits of the significant range of frequencies are: $2.7288 \leqslant \Omega \leqslant 122.806$.

skeptical readers reading this paper we demonstrate three basic steps on the reading of microcurrents that were described above. Not having much place for the detailed analysis of these microcurrents we forced to show only few figures that demonstrate the power of new spectroscopy based on the NAFASS.

Step 1. The extraction of the optimal trend based on the POLS.

The Figs. 8a and 8b demonstrate the optimal smoothing procedure applied to the integrated curve. The differentiation of the optimal trend (shown for the integrated curve by solid line) gives the optimal trend (the value of the optimal smoothing window $w_{opt} = 0.03$). Differentiation of the optimal trend calculated for the integrated curve gives the optimal trend for the initial sequence. It is shown on Fig. 8b by blue solid line. As one can notice from these figures we chose the segment with large value of the spontaneous microcurrent (signal) that is considered as a neurophysiologic reaction of membrane.

Step2. The key point of the fluctuation metrology is based on the NAFASS approach that enables to "read" any smoothed trend and express it in terms of the corresponding AFR. We want to

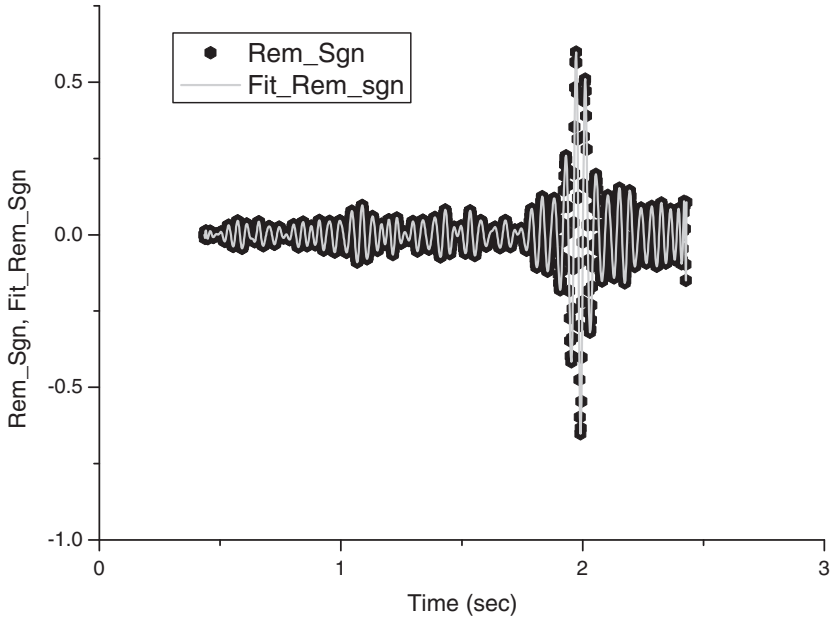

Fig. 9c. Here we show the fit of the remnant function "Rem_Sgn" shown above on Fig. 9a. This function has own AFR (2) (see Fig. 9d) and it is totally different from the AFR (1) shown on Fig. 9b.

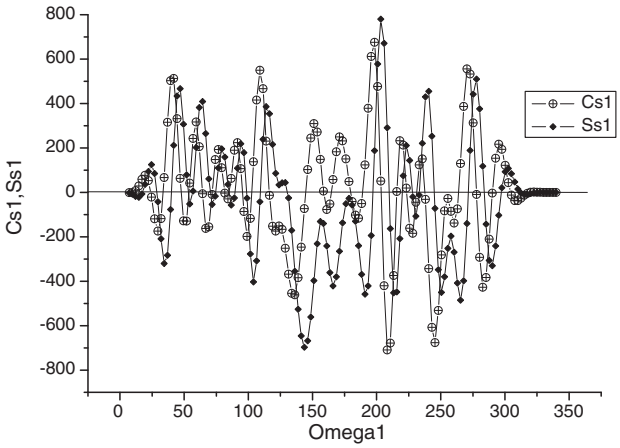

Fig. 9d. Here we show the non-monotonic behavior of the AFR (2) obtained in the frame of the NAFASS approach for the "Rem_Sgn" data file depicted on the previous Fig. 9c. As one can notice from a brief analysis the significant frequency band is increased approximately in three times in order to provide the satisfactory fit (RelErr = 10.1125%) of this remnant function. The limits of the significant range of frequencies for the AFR (2) are: $7.167 \leqslant \Omega 1 \leqslant 339.858$.

stress here that the informative-significant frequency band found in the frame of the NAFASS cannot coincide with conventional Fourier spectrum because it uses the *limited* band minimizing the frequency "distance" ($\Omega_{max} - \omega_{min}$). For this specific case on Fig. 9a we show the fit of the optimal trend (depicted previously on Fig. 8b) and its AFR (1) (Fig. 9b). Besides this possibility in the frame of the NAFASS one can fit the remnant function defined by Eq. (35) and find also its AFR (2). It opens quite new possibilities in interpretation and calibration of these discrete and limited spectra associated with of the optimal trend and the remnant function. The fit of the remnant function is shown on Fig. 9c and the corresponding AFR (2) on 9d. As it can be seen from the brief analysis of Fig. 9d the AFR (2) of the remnant function describes the high-frequency spectrum that was not contained in the AFR (1) describing the optimal trend (compare with 9b).

Step.3. In order not to miss any information that are contained in the random sequence the detrended "noise" (defined here as the initial remnant function $Rem(y)$) can be read also and expressed in terms of the β-distribution [43]. The fit of the detrended noise is shown by Fig. 10a and (b).

The basic quantitative parameters describing these biological data are collected in Table 3.

So, after realization of these three simple but important steps we obtain new quantitative "alphabet" (AFR (1), AFR (2) and 4 parameters belonging to β-distribution). They are necessary for comparison of the sequence analyzed with others. Definitely, any parameters of a model noise can be read also in terms of this "universal" quantitative language. For translation of the specific qualitative properties of the model noise considered (as its "color" (white and etc.), affiliation to a certain class of distributions (Gauss, Student, Fisher and etc.), self-similarity (fractal) properties and etc.) it is necessary to create in the nearest future a

Table 3
The fitting parameters describing the β-distribution $B(t) = B_0(t - t_0)^{\alpha}(t_N - t)^{\beta} + D$.

Number of the β-distr	B_0	α	β	D	$B_{max}t_{max}$	RelErr (%)
1	0.6219	0.71098	0.66269	0.00573	0.62675 1.46832	0.91295

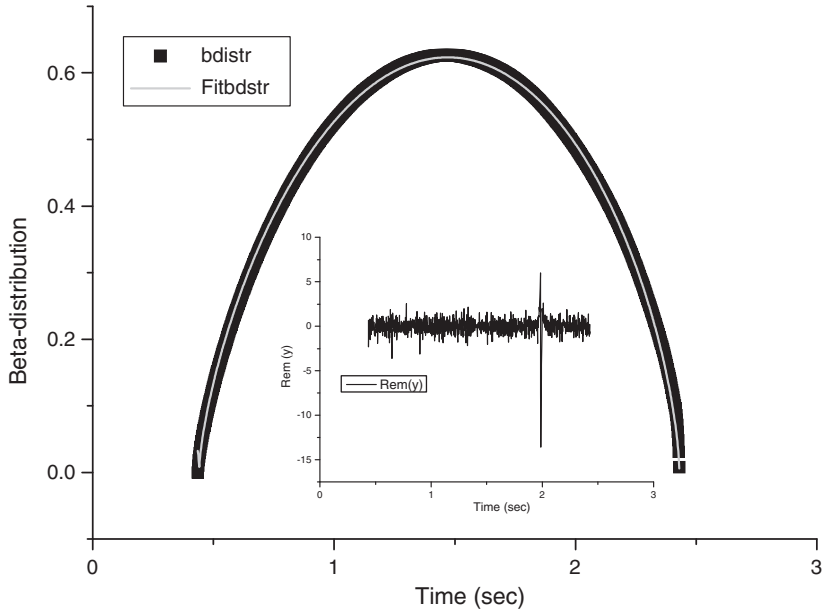

Fig. 10a. The fit of the initial remnant function $Rem(y)$ (shown inside the small frame) to the β-distribution function. Details of the transformation are presented in paper [43]. The fitting parameters are collected in Table 3. Comparing this figure with Fig. 7b one can say that the detrended noise can be read in terms of the fitting parameters belonging to the ACF or β-distribution, correspondingly.

specific vocabulary as it has been accepted for communications and understanding between carriers of different languages.

We hope also that these fitting parameters forming a "universal" language for reading and classification of different fluctuations can be used in the nearest future as the basic metrological parameters for the *modeless* description of different random sequences belonging to different sources of their generation (medical, technical, geological, chemical astrophysical and etc.).

Acknowledgements

One of the authors (RRN) expresses his thankfulness to Prof. Dr. Ali Osman Solak (NIR data, Ankara University, Turkey) and Dr. A. Skorinkin (Neuro data, department of bioelectronics, Kazan Federal University) for possibility to use their data for this kind of analysis. All authors express their sincere acknowledgements for the grant (number of grant 1.84.11) of the Ministry of Higher Education and Science of the Russian Federation for its financial support.

References

[1] Champeney DC. Handbook of fourier theorems. Cambridge: Cambridge University Press; 1987.
[2] Goldberg RR. Fourier transforms. Cambridge University Press; 1965.
[3] H. Nelson, Harmonic Analysis, The Wadsworth & Brooks, Cole Mathematics Series, Addison-Wesley, 1983, reprinted by Wadsworth, 1991.
[4] Y. Katznelson, An Introduction to Harmonic Analysis, John Wiley and Sons, 1968, reprinted by Dover, new York, 1976.
[5] Stein EM, Weiss G. Introduction to Fourier analysis on euclidean spaces. Princeton University Press; 1971.
[6] Titchmarsh EC. Introduction to the theory of Fourier integrals. second ed. Oxford University Press; 1948.
[7] Zygmund A. Trigonometric series. second ed. Cambridge University Press; 1959.
[8] Beylkin G, Coifman R, Daubechies I, Mallat S, Meyer Y, Raphael L, et al., editors. Wavelets and Their Applications. Cambridge, MA: Jones and Bartlett; 1992.
[9] Chui CK, editor. Approximation Theory and Functional Analysis. Boston: Academic Press; 1991.
[10] Chui CK. Wavelets: a tutorial in theory and applications. Boston: Academic Press; 1992.
[11] Combes JM, Grossmann A, Tchamitchian P, editors. Wavelets: Time-Frequency Methods and Phase Space. New York: Springer-Verlag; 1991.
[12] I. Daubechies, Wavelets, CBMS-NSF Series in Appl.Math., SIAM Publ., Philadelphia, 1992.
[13] A.V. Oppenheim and R.W. Schafer, Discrete-Time Signal Processing, Prentice Hall Signal Proc. Series, Prentice Hall, Englewood Cliffs, New Jersey, 1989.
[14] C.K. Chui, and G. Chen, Signal Processing and Systems Theory-Selected Topics, Springer Series in Information Sciences, v.26, Springer-Verlag, New York, 1991.
[15] Osborne MR. Some special nonlinear least squares problems. SIAM J Numer Anal 1975;12:571.
[16] Kay SM, Marple SI. Spectrum analysis – a modern perspective. Proc IEEE 1981;69:1380.
[17] G.K. Smyth, Coupled and Nested Iterations in Nonlinear Estimation. PhD Thesis, Australian National University, Canberra.
[18] Brester Y, Macovski A. Exact maximum likelihood parameter estimation of superposed exponential signals in noise. IEEE Trans Acoust Speech Signal Process 1986;34:1081.
[19] Osborne MR, Smyth GK. A modified Prony algorithm for fitting functions defined by difference equations. SIAM J Sci Stat Comput 1991;12:362.
[20] Kahn M, Mackisack MS, Osborne MR, Smyth GK. On the consistency of Prony's method and related algorithms. J Comput Graphical Stat 1992;1:329.
[21] Kundu D. Estimating the parameters of undamped exponential signals. Technometrics 1993;35:215.
[22] Mackisack MS, Osborne MR, Smytth GK. A modified Prony algorithm for estimating sinusoidal frequencies. J Stat Comput Simul 1994;49:11–124.
[23] Kundu D. Estimating the parameters of complex-valued exponential signals. Comput Statist Data Anal 1994;18:525–34.
[24] Kannan N, Kundu D. On modified EVLP and ML methods for estimating superimposed exponential signals. Signal Process 1994;39:223–33.
[25] Osborne MR, Smyth GK. A modified Prony algorithm for fitting sums of exponential functions. SIAM J Sci Stat Comput 1995;16:119–38.
[26] Smyth GK, Hawkins DM. Robust frequency estimation using elemental sets. Comput Sci Stat 1997;28:659–62.
[27] Smyth GK, Hawkins DM. Robust frequency estimation using elemental sets. J Comput Graphics Stat 2000;9:196–214.
[28] Smyth GK. Employing constraints for improved frequency estimation by eigen-analysis method. Technometrics 2000;42:277–89.
[29] Merlet JP. Singular configurations of parallel manipulators and Grassman geometry. Int J Rob Res 2000;19:271–88.
[30] Golub GH, Milanfar P, Varah J. A stable numerical method for inverting shape from moments. SIAM J Sci Comput 1999;21:1222–43.
[31] Nigmatullin RR, Alekhin AP, Baleanu D, Dinch E, Ustundag Z, Ekshi H, et al. Analysis of the effect of the potential cycles of the reflected infrared signals of nitro groups in nanofilms: application of the Fractional Moments Statistics. Electroanalysis 2010;22:419.
[32] Nigmatullin RR, Baleanu D, Dinch E, Ustundag Z, Solak AO, Kargin RV. Analysis of a nanofilm of the mercaptophenyl diazonium modified gold electrode within new statistical parameters. J Comput Theor Nanosci 2010;7:1.
[33] Nigmatullin RR, Baleanu D, Dinch E, Solak AO. Characterization of a benzoic acid modified glassy carbon electrodes expressed quantitatively by new statistical parameters. Physica E 2009;41:609.
[34] Nigmatullin RR. Strongly correlated variables and existence of the universal distribution function for relative fluctuations. Phys Wave Phenom 2008;16(2):119.
[35] Nigmatullin RR, Le Mehaute A. Is there a geometrical/physical meaning of the fractional integral with complex exponent? J Non-Cryst Solids 2005;351:2888.
[36] Nigmatullin RR. Theory of dielectric relaxation in non-crystalline solids: from a set of micromotions to the averaged collective motion in the mesoscale region. Phys B: Phys Condens Matter 2005;358:201.
[37] Nigmatullin RR. Eigen-coordinates: new method of identification of analytical functions in experimental measurements. Appl Magn Reson 1998;14:601.
[38] Nigmatullin RR. Recognition of nonextensive statistic distribution by the eigen-coordinates method. Physica A 2000;285:547.
[39] Al-Hasan M, Nigmatullin RR. Identification of the generalized weibull distribution in wind speed data by the eigen-coordinates method. Renewable Energy 2003;28:93.
[40] Nigmatullin RR, Smith G. Fluctuation-noise spectroscopy and a 'universal' fitting function of amplitudes of random sequences. Physica A 2003;320:291.
[41] M.G. Kendall and A. Stuart, The advanced theory of statistics, vol.1 (Distribution theory) Ch. Griffin & Company Limited, London, 1965.
[42] Goncharov VA. Estimation of correlation functions in dielectric thermal-noise measurements: variable RC-circuit approach. J Non-cryst Solids 2002;305:59.
[43] Nigmatullin RR. Universal distribution function for the strongly-correlated fluctuations: general way for description of random sequences. Commun Nonlinear Sci Numer Simul 2010;15:637–47.
[44] Nigmatullin RR, Popov II, Baleanu D. Predictions based on the cumulative curves: basic principles and nontrivial example. Commun Nonlinear Sci Numer Simul 2011;16:895–915.
[45] Timashev SF, Polyakov YuS, Lakeev SG, Misurkin PI, Danilov AI. The principles of fluctuation metrology. J Phys Chem 2010;84:1980. in Russain.